Acta Biologica Hungarica 59 (Suppl.), pp. 81–92 (2008)
DOI: 10.1556/ABiol.59.2008.Suppl.13

IMMUNOHISTOLOGICAL STUDIES ON THE DISTRIBUTION OF LEARNING-RELATED PEPTIDES IN THE CENTRAL NERVOUS SYSTEM OF CONDITIONED *LYMNAEA**

Y. NOMURA,[1] D. HATAKEYAMA,[2] T. HORIKOSHI[3] and M. SAKAKIBARA[3]**

[1] Course of Biological Science and Technology, Graduate School of High-Technology for Human Welfare, Tokai University, 317 Nishino, Numazu 410-0321, Shizuoka, Japan
[2] Dept.8.3-Biosciences, Zoology/Physiology, Natural Sciences and Technology III, Saarland University, Postfach 151150, D-66041 Saarbrücken, Germany
[3] Department of Biological Science and Technology, School of High-Technology for Human Welfare, Tokai University, 317 Nishino, Numazu 410-0321, Shizuoka, Japan

(Received: October 22, 2007; accepted: December 7, 2007)

Behavioral conditioning in *Lymnaea* increased the amount of immunolabeling in the central nervous system for the memory-associated protein calexcitin. The staining level of anti-calexcitin positive neurons was always stronger in conditioned animals than in naïve animals. In the visuo-vestibular conditioned animals, right-parietal and visceral group neurons as well as withdrawal-related neurons were positively stained with anti-calexcitin antibody. In taste-aversion conditioned animals, right-parietal visceral G-group neurons and withdrawal-related neurons were selectively stained. These neurons are candidate neurons for modulation by these conditioning paradigms.

Keywords: Calexcitin – visuo-vestibular conditioning – taste-aversion conditioning – immunohistochemistry – whole-body withdrawal response

INTRODUCTION

Our previous studies demonstrated that *Lymnaea* can be classically conditioned with two different paradigms; visuo-vestibular conditioning (VVC) [12, 16] and taste aversion conditioning (TAC) [8]. The unconditioned response of both paradigms is a whole-body withdrawal response. Although the VVC paradigm is the same as that for *Hermissenda* [1], the neuronal circuit for sensing and processing visual and vestibular information is different [15, 17], and the underlying neural pathways of the classical conditioning are also suggested to be different [14]. The underlying neu-

* Presented during the 11th ISIN Symposium on Invertebrate Neurobiology, 25–29 August, 2007, Tihany, Hungary

** Corresponding author; e-mail: manabu@tokai.ac.jp

0236-5383/$ 20.00

ronal mechanisms of withdrawal response involved these conditioning paradigms in *Lymnaea* are not yet fully established. Therefore, we attempted to elucidate the neural circuits of these conditioning paradigms in *Lymnaea* using the conditioning-specific marker protein calexcitin (CE). Calexcitin, a 22 kD GTP-binding protein, was originally found in its phosphorylated form in the type B photoreceptor of Pavlovian classically-conditioned *Hermissenda* [2]. This protein, which binds Ca^{2+}, targets ryanodine receptors on the endoplasmic reticulum and triggers the release of Ca^{2+} from internal stores while concurrently reducing voltage-dependent K^+ currents, i.e. I_A and $I_{Ca^{2+}\text{-}K^+}$ [3, 4, 11]. Calexcitin immunostaining of the B photoreceptor in conditioned *Hermissenda* is more intense than that in animals receiving random presentations of the conditioning stimulus (CS) and unconditioning stimulus (UCS), or in naïve, unconditioned animals. The intensity of the immunostaining correlates to the level of short- and long-term memory demonstrated by the animals [9, 10]. Calexcitin is a protein kinase C substrate in the *Lymnaea* central nervous system, as demonstrated by a previous immunohistologic study [7]. We compared the immunohistologic distribution of anti-CE positive neurons in conditioned and control (naïve and pseudo-random) *Lymnaea* preparations.

MATERIAL AND METHODS

Animals

Laboratory-reared freshwater pond snails, *Lymnaea stagnalis* (original stocks from Free University of Amsterdam or supplemented with snails from Hokkaido University or University of Calgary that were derived from the same Amsterdam colony) with shell lengths of 20 mm, were maintained at 20 °C in well-aerated water, on a 12 h light:12 h dark cycle (on at 08:00 AM), and fed cabbage and goldfish pellets. The animals were food-deprived for 24 h prior to the experiments.

Visuo-vestibular conditioning

Methods for VVC were described in detail previously [12, 16]. In brief, animals were dark-adapted for 15 min prior to training. Each animal was kept in a freshwater-filled cell culture flask fixed on an orbital shaker and placed in a sound- and light-proof incubator maintained at 20 °C. Prior to conditioning, animals were screened to determine whether they responded to the onset of a light flash as a pre-conditioning test. Then, a 3 s light flash of 700 $\mu W/cm^2$ at 500 nm at the surface of the flask as the conditioning stimulus 1 (CS1) was delivered through a light guide onto the shaker and orbital rotation with a 4 mm orbital shaking motion at 1960 rpm was presented using the orbital shaker as the unconditioning stimulus 1 (UCS1) with a 1-s delay from the onset of CS1 and terminated simultaneously with CS1. Thirty pairings of CS1 and UCS1 were presented with 2 min inter-trial intervals within 1 d. Pseudo-

random controls were animals that received the same number of non-overlapping CS1 and UCS1 exposures at random intervals. Following the conditioning, in response to a light flash, the animals showed whole-body withdrawal behavior, which was the unconditioned response 1 (UCR1) to UCS1. A retention test was performed at 15 min and 24 h after completing the conditioning to determine whether the animals had a withdrawal response to CS1 presentation. The retention test 24 h after the conditioning (24 h post-conditioning test) was performed three times with 2 min inter-trial intervals. Animals that showed a withdrawal response to CS1 presentation in at least one of the three tests were considered to have acquired memory for the conditioning and were used for further immunohistologic examination.

Taste-aversion conditioning

The experimental apparatus and conditioning methods for TAC were described in detail previously [8]. In brief, a Plexiglas container had a perfusion system with one inlet and one outlet pipe from which the solution inside the container could be entirely replaced within 30 s at a speed of 250 ml/min. The container always contained 10 ml fresh water. To observe the feeding response, a mirror was placed under the container. A taste stimulus of 1 ml of 100 mM sucrose was applied directly to the lip of the animal with a 1 ml syringe. A tactile stimulus was applied to the surface of the animal's head using a hand-held Plexiglas rod. The tactile stimulation was strong enough to always evoke a whole-body withdrawal response in addition to cessation of the spontaneous feeding response. After 10 min adaptation in the container, the feeding response to sucrose was recorded as a pre-conditioning test. Ten minutes after the pre-conditioning test, the animals received 20 pairings of conditioning stimuli. Animals were exposed to paired presentations of sucrose (CS2) for 5 s, followed 5 s later by tactile stimulation (UCS2). One-minute inter-trial intervals were selected because animals required less than 1 min to recover from the withdrawal response caused by UCS2. Pseudo-random control animals received the same number of exposures of sucrose application and tactile stimulation in random order. A post-conditioning test was performed with sucrose application 10 min after the conditioning. A memory retention test was performed 24 h later. A good performer was defined as an animal that had a significantly reduced feeding response to sucrose application at the 24 h post-conditioning test. Good performers and pseudo-random controls were assessed immunohistologically.

Preparations and immunohistochemistry

Immediately after the 24 h post-conditioning test, the circumesophageal ganglion complex was quickly dissected out from each animal in *Lymnaea* saline (51.3 mM NaCl, 1.7 mM KCl, 5.0 mM $MgCl_2$, 1.5 mM $CaCl_2$ and 5.0 mM HEPES, pH 7.9–8.1) and pinned to a Sylgard-coated Petri dish, and covered with fixative. Preparations

were fixed in 4% paraformaldehyde diluted in 0.1 M phosphate buffer, dehydrated in an ethanol series, and embedded in paraffin. Serial 4-μm sections were cut horizontally using a microtome (ERM-1017, Erma Inc., Tokyo, Japan). Thin paraffin sections were washed thoroughly with phosphate-buffered saline (PBS) containing 0.05% Triton X-100, and then processed for immunohistochemistry. The preparations were incubated with primary anti-CE antibody (a kind gift from Dr. Tom Nelson of Blanchette Rockefeller Neuroscience Institute, Morgantown, WV) diluted 1 : 25,000 in PBS at 4 °C overnight. The preparations were washed in PBS for 10 min 3 times and incubated in a 1 : 150 dilution of biotin-labeled secondary antibody (goat anti-rabbit-IgG antibody; Vector Laboratories, Burlingame, CA) in PBS at room temperature for 30 min. Avidin-biotin-peroxidase complex reagent (ABC methods; Vector Laboratories) was then applied to the preparations at room temperature for 60 min. Finally, peroxidase activity was visualized by 3-min incubation with 0.1% 3,3'-diaminobenzidine in 50 mM Tris-HCl buffer (pH 7.5) supplemented with 0.02% H_2O_2. After rinsing with 50 mM Tris-HCl buffer, the preparations were dehydrated in a 70%–100% ethanol series, cleared in xylene, and mounted in Eukitt mounting medium for light microscopic examination. Serial sections were examined using a light microscope (Optiphoto-2, Nikon, Tokyo, Japan) and the images were captured with a digital camera system (DP20, Olympus, Tokyo, Japan). The immunostaining levels of each section were analyzed using the image processing software "Scion Image" (Scion Corp., Frederick, MD). The distribution ratio shown in Table 1 was defined as the ratio of anti-CE positive neurons observed in one conditioning paradigm to the total number of animals examined in the same conditioning paradigm. Though the nomenclature of neurons in each ganglion is based on previous studies [5, 6, 13, 18], cells identified for the first time in this study were termed "no name settled (NNS)". All chemicals, unless otherwise mentioned, were purchased from Sigma-Aldrich Chemical Co. (St. Louis, MO).

RESULTS

We examined the immunohistologic CE distribution in 20 animals of each of the naïve, VVC, TAC, pseudo-random TAC control groups, and 5 pseudo-random VVC controls.

Distribution of anti-CE positive neurons in naïve animals

In naïve animals, anti-CE positive neurons were observed in the cerebral, pedal, parietal and visceral ganglia. Though there was faint staining of the surrounding neurons, the staining in the cytosol of the neurons in these ganglia was uniform (Fig. 1). A few, but not all dorsolateral cerebral or pedal A-cluster neurons were anti-CE positive; dorsolateral cerebral neurons were anti-CE positive in 85% of the animals; pedal A-cluster neurons were anti-CE positive in 40% of the 20 animals we exam-

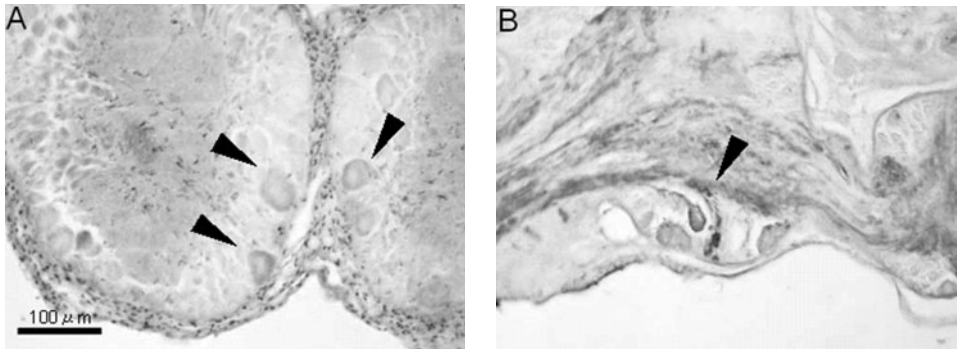

Fig. 1. Anti-CE positive neurons in naïve animals. A. Five pedal A-cluster neurons had anti-CE positive signals, three of these are indicated with arrowheads. Although the extent of staining was low, the cytosolic signal was uniform. B. Anti-CE positive neurons in the cerebral A-cluster

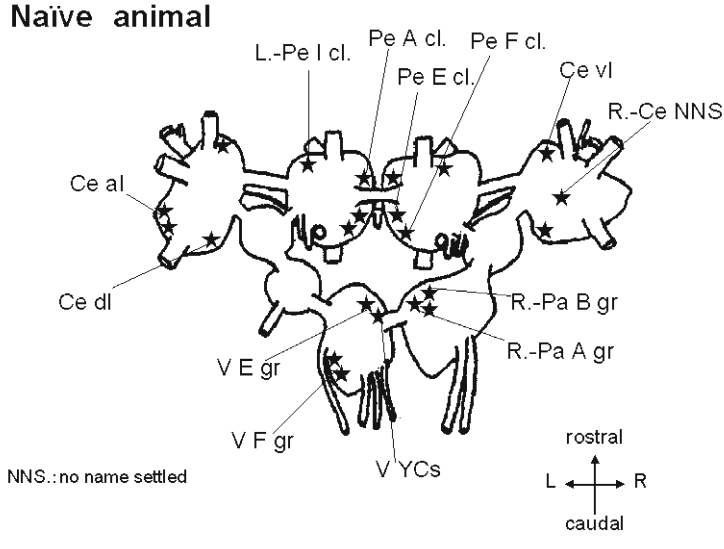

Fig. 2. Distribution of anti-CE positive neurons in naïve animals. Not all neurons within a cluster had positive signals, rather only a few cells were stained. This diagram was drawn based on the results of 20 animals. At least one preparation for each animal was stained

ined. In some cases, the anti-CE positive neurons were distributed in the pedal E- (25%) and F- (25%) clusters; in the right parietal A- (35%) and B- (45%) clusters; and in the visceral E- (30%) and F- (20%) clusters. Figure 2 summarizes the locations of the anti-CE positive neurons observed in the naïve central nervous system.

Distribution of anti-CE positive neurons in VVC animals

Although all animal groups (naïve, VVC, TAC and the pseudo-random controls) had some dorsolateral cerebral and pedal E-, F- and A-cluster neurons that were anti-CE positive, the distribution ratio of anti-CE positive neurons was different between the

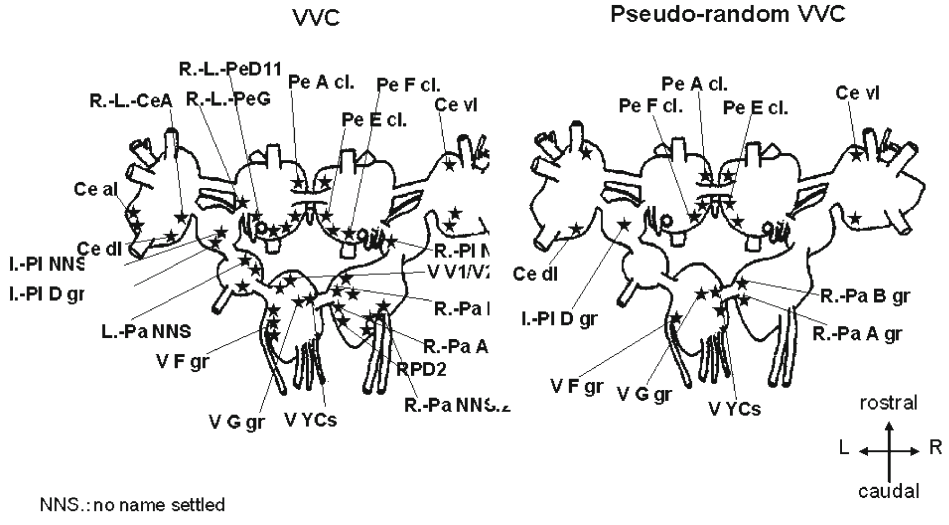

Fig. 3. Right-panel: Distribution of anti-CE positive neurons in 20 VVC animals. Left-panel: Distribution of anti-CE positive neurons in 5 pseudo-random VVC control animals.
For abbreviations see Table 1

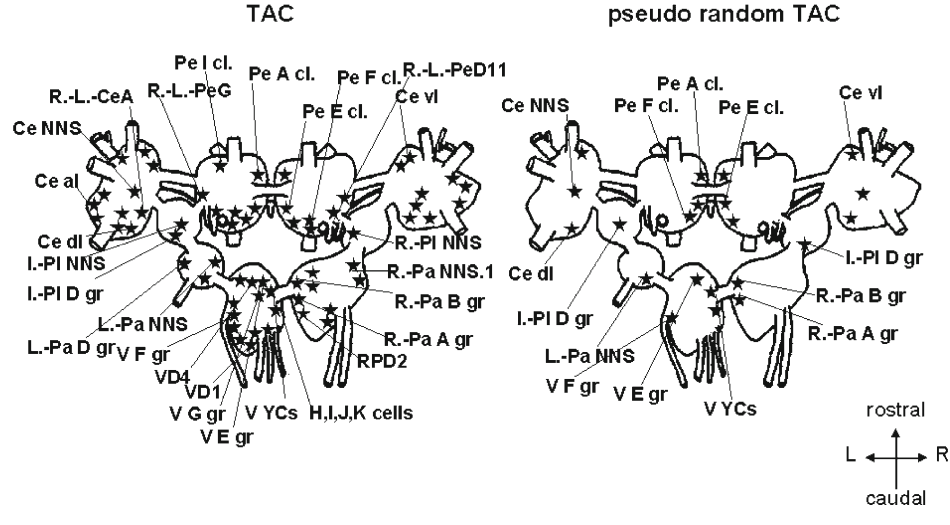

Fig. 4. Right-panel: Distribution of anti-CE positive neurons in 20 TAC animals. Left-panel: Distribution of anti-CE positive neurons in 20 pseudo-random TAC control animals.
For abbreviations see Table 1

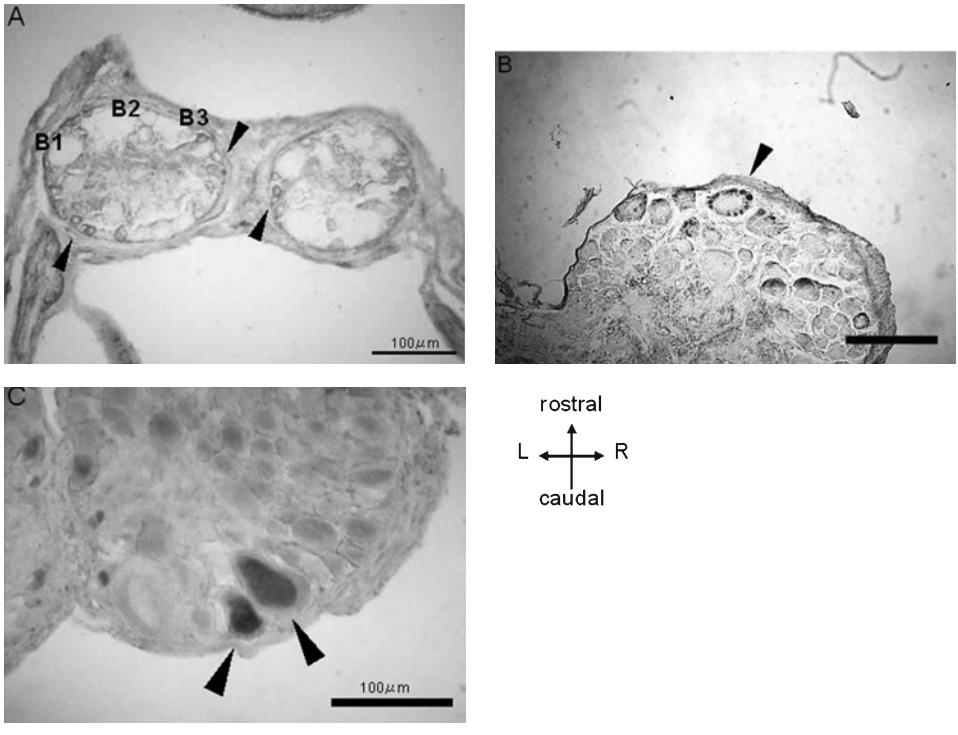

Fig. 5. Characteristic staining was observed in TAC animals. Animals were behaviorally confirmed to have good memory at the 24 h post-conditioning test. A. No anti-CE positive signal was detected in B1, B2 and B3 motoneurons in the buccal ganglion, which are related with feeding behavior. Small neurons comprising the central pattern generator indicated by arrowheads have strong immunohistologic signals. B. Selective staining in TAC animal was observed; the extent of staining was not restricted to the cytosol, but appeared as a ring-like structure. C. The anti-CE signal is obvious in nuclei of neurons in the right parietal ganglion at 48 h after conditioning

VVC group and the pseudo-random controls; dorsolateral cerebral neurons (100% in VVC vs 60% Right/40% Left in controls); pedal A-cluster neurons (75% in VVC vs 60% in controls). The distribution of anti-CE positive neurons in the VVC and VVC pseudo-random control groups is summarized in Fig. 3. The degree of staining in animals that received paired conditioning was always stronger than that in the naïve controls.

Distribution of anti-CE positive neurons in TAC animals

The dorsolateral cerebral neurons in TAC animals had a greater anti-CE positive staining density than those in naïve animals. Furthermore, there was selective staining of the pedal LPeD11 and F-cluster neurons, and the parietal and pleural NNS

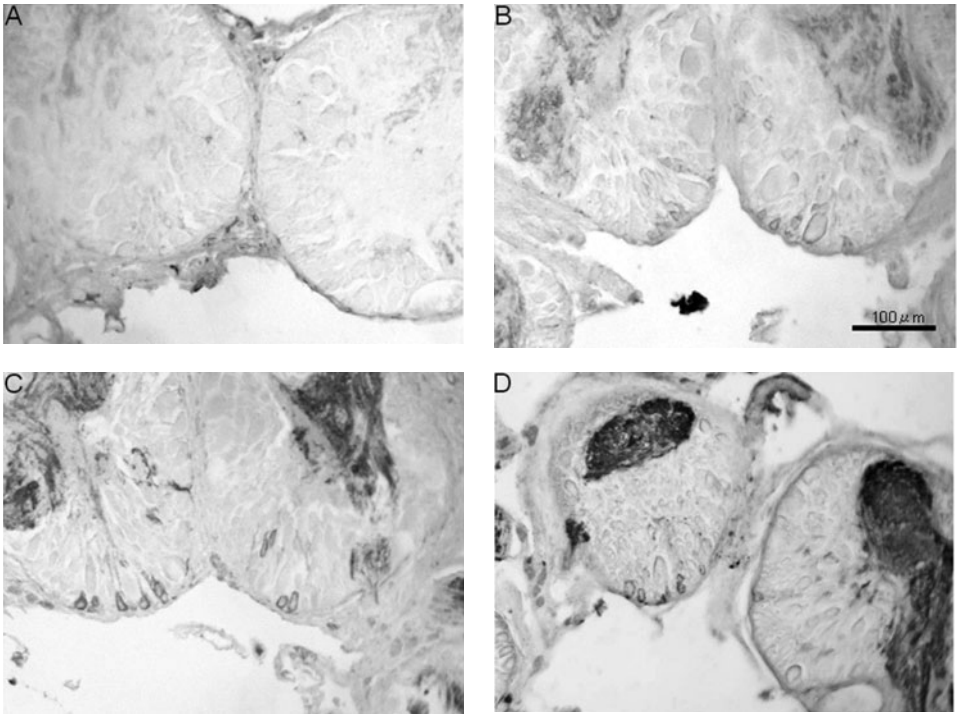

Fig. 6. The dynamic nature of immunohistologic signals in the pedal E- and F-clusters. A. Soon after the TAC, no positive signal was detected. The 10 min post-conditioning test indicated that this animal had good memory for the CS2 presentation. B. Three hours after TAC, positive signals at the E- and F-clusters were obvious. The animals underwent a memory retention test to confirm good memory prior obtaining the tissue for the immunohistochemistry shown in B, C and D. C. Six hours after TAC, a more dense signal was detected in the same area. D. This image was obtained 48 h post-TAC

Table 1
Distribution ratio of well-stained neurons with anti-CE antibody in each conditioning paradigm

Cerebral ganglia	Distribution ratio of anti-CE positive neurons				
	TAC[1]	TAC random[1]	VVC[1]	VVC random[2]	Naïve[1]
R-Cerebral dl	1.00	0.75	1.00	0.60	0.85
L-Cerebral dl	1.00	0.75	1.00	0.40	0.85
R-Cerebral vl	0.40	0.05	0.10	0.20	0.30
L-Cerebral vl	0.40	0.10	0.00	0.20	0.15
R-Cerebral al	0.55	0.00	0.05	0.00	0.00
L-Cerebral al	0.35	0.00	0.30	0.00	0.00
R-CeA	0.30	0.00	0.30	0.00	0.00
L-CeA	0.20	0.00	0.25	0.00	0.00
R-Cerebral NNS[3]	0.80	0.10	0.40	0.00	0.25
L-Cerebral NNS[3]	0.55	0.25	0.00	0.00	0.00

Table 1 (cont.)

Cerebral ganglia	Distribution ratio of anti-CE positive neurons				
	TAC[1]	TAC random[1]	VVC[1]	VVC random[2]	Naïve[1]
Pleural					
R-Pleural D group	0.00	0.20	0.00	0.00	0.00
L-Pleural D group	0.35	0.20	0.30	0.40	0.00
R-Pleural NNS[3]	0.45	0.00	0.35	0.00	0.00
L-Pleural NNS[3]	0.40	0.00	0.20	0.00	0.00
Pedal					
Pedal A cluster	0.85	0.20	0.75	0.60	0.40
Pedal E cluster	0.75	0.45	0.45	0.40	0.25
Pedal F cluster	0.75	0.25	0.35	0.20	0.25
L-Pedal I cluster	0.15	0.00	0.00	0.00	0.10
R-PeD11	0.40	0.00	0.00	0.00	0.00
L-PeD11	0.40	0.00	0.10	0.00	0.00
R-PeG	0.40	0.00	0.00	0.00	0.00
L-PeG	0.25	0.00	0.30	0.00	0.00
Parietal					
R-Parietal A group	0.75	0.25	0.50	0.20	0.35
Parietal B group	0.65	0.40	0.70	0.60	0.45
RPD2	0.40	0.00	0.05	0.00	0.00
L-Parietal D group	0.60	0.00	0.05	0.00	0.00
R-Parietal NNS1[3]	0.45	0.00	0.00	0.00	0.00
R-Parietal NNS2[3]	0.00	0.00	0.55	0.00	0.00
L-Parietal NNS[3]	0.30	0.20	0.35	0.00	0.00
Visceral					
Visceral V1/V2	0.00	0.00	0.55	0.00	0.00
Visceral E group	0.40	0.25	0.00	0.00	0.30
Visceral YCs	0.40	0.35	0.45	0.20	0.25
Visceral F group	0.70	0.15	0.60	0.40	0.20
Visceral G group	0.35	0.00	0.25	0.20	0.00
H, I, J, K cells	0.35	0.00	0.00	0.00	0.00
VD1	0.25	0.00	0.00	0.00	0.00
VD4	0.10	0.00	0.00	0.00	0.00
Visceral NNS[3]	0.00	0.00	0.35	0.00	0.00

R: right; L: left; cerebral dl, dorsolateral cerebral; cerebral vl, ventrolateral cerebral; cerebral al, anterolateral cerebral; TAC: Taste-Aversion Conditioning; TAC random: pseudo-random TAC control animals; VVC: Visuo-Vestibular Conditioning; VVC random : pseudo-random VVC control animals; [1] out of 20 animals; [2] out of 5 animals; [3] NNS: no name settled neuron.

neurons only in the conditioned animals (Fig. 4). Remarkably, selective anterolateral cerebral, cerebral A-cluster, PeD11, and G-cluster neurons on both the right and left sides were anti-CE positive only in conditioned animals, and not in the pseudo-random or naïve animals. Anti-CE positive neurons were distributed in every ganglion in the pseudo-random controls, but the number of anti-CE positive neurons was much higher in the conditioned animals. Dorsolateral cerebral and right cerebral NNS neurons were always darkly stained in every preparation. The number of stained neurons within the clusters of the pedal ganglion increased after the conditioning. Although motor neurons in the buccal ganglia, such as B1, B2 and B3, were not completely stained after the conditioning (Fig. 5A), there was good contrast with the clear positive signals in the small neurons comprising the central pattern generator in the buccal ganglia. The staining of these small neurons was not restricted to cytosol, but rather formed a ring-like structure (Fig. 5B) as reported previously [7]. The dynamic nature of the immunohistologic signal changed as a reflection of robust memory formation (Fig. 6). Soon after the conditioning, we could not detect any anti-CE positive signals in the pedal E- and F-clusters (Fig. 6A), although the animals had good memory, as revealed in the 10 min post-conditioning test. The immunohistologic signal became stronger 3 and 6 h after conditioning (Fig. 6B, C, respectively). The signal was even stronger in the conditioned animals at 48 h (Fig. 6D). In some cases, the immunohistologic signal moved into the nucleus from the cytosol (Fig. 5C).

Table 1 summarizes the distribution of anti-CE positive neurons in each conditioning group and in the naïve animals.

DISCUSSION

We immunohistologically identified conditioning-specific neurons using the PKC substrate memory protein CE; visceral V1, V2 and NNS neurons, and right parietal NNS2 neurons were selectively stained following VVC; visceral G-group, H, I, J, K, VD1 and VD4 neurons, and right parietal NNS1 neurons were stained following TAC conditioning. In contrast, in naïve animals, both the right and left dorsolateral and ventral cerebral neurons; the pedal A-, E- and F-cluster neurons; the parietal A- and B-group cluster neurons; and the visceral E-, F- and Y-group cluster neurons were anti-CE positive.

The distribution of anti-CE positive neurons in the naïve animals was consistent with previous findings, even in frozen thick preparations. Our previous study demonstrated anti-CE positive neurons in naïve *Lymnaea* in two ganglia; in the cerebral ganglia, CE-like immunoreactivity was present in two pairs of cell clusters that receive taste signals from the superior or median lip nerves, and in the pedal ganglia, CE-like immunoreactivity was detected in 1 to 4 cells of the pedal A-clusters, which are involved in the withdrawal response [7]. Anti-CE positive neurons are assumed to be naturally present in PKC-specific phosphorylated pathways in naïve animals. The immunoreactive signals were always stronger in the conditioned animals than in

the naïve animals. This finding suggests that key neurons in the neuronal pathways involved in conditioning in both paradigms are phosphorylated by PKC, as previously suggested in *Hermissenda* [9, 10].

Neurons that were anti-CE positive in both VVC and TAC animals are assumed to be conditioning-specific withdrawal neurons. These were the anterolateral cerebral and cerebral A-cluster neurons; L-PeD11, L-PeG, parietal RPD2, parietal D-group, and NNS1 and NNS2 neurons; and right and left pleural NNS neurons. Among these neurons, the right and left cerebral A-cluster, L-PeG and L-PeD11 neurons are involved in the withdrawal response [18].

After TAC acquisition, animals tend to inhibit their feeding response to sucrose (CS2), therefore neurons with positive immuno-signals in TAC animals, but not pseudo-random controls, are assumed to be the neurons involved in the specific feeding response, and are the visceral G-group and parietal R-NNS1 neurons, but not the visceral H, I, J, K, VD1 and VD4 neurons, which are withdrawal-related neurons.

Neurons that are anti-CE positive only in VVC animals and not in the pseudo-random controls are assumed to be the neurons modulated by VVC; these are the visceral NNS and parietal R-NNS2 neurons, but not the withdrawal-related visceral V1/V2 neurons. Because in this study we only examined the PKC-mediated calexcitin-dependent signaling pathway, pathways involving another second messenger system, such as PKA and CaM kinase, as in the *Aplysia* system, cannot be ruled out. In future studies, we will evaluate the role of these conditioning-specific neurons using electrophysiologic methods.

REFERENCES

1. Alkon, D. L. (1987) *Memory Traces in the Brain*. Cambridge University Press, Cambridge, London, New York, Rochelle, Melbourne, Sydney.
2. Alkon, D. L., Nelson, T. J. (1990) Specificity of molecular changes in neurons involved in memory storage. *Faseb J. 4,* 1567–1576.
3. Alkon, D. L., Nelson, T. J., Zhao, W., Cavallaro, S. (1998) Time domains of neuronal Ca^{2+} signaling and associative memory: steps through a calexcitin, ryanodine receptor, K^+ channel cascade. *Trends Neurosci. 21,* 529–537.
4. Ascoli, G. A., Luu, K. X., Olds, J. L., Nelson, T. J., Gusev, P. A., Bertucci, C., Bramanti, E., Raffaelli, A., Salvadori, P., Alkon, D. L. (1997) Secondary structure and Ca^{2+}-induced conformational change of calexcitin, a learning-associated protein. *J. Biol. Chem. 272,* 24771–24779.
5. Elekes, K., Eckert, M., Rapus, J. (1993) Small sets of putative interneurons are octopamine-immunoreactive in the central nervous system of the pond snail, *Lymnaea stagnalis*. *Brain Res. 608,* 191–197.
6. Ferguson, G. P., Benjamin, P. R. (1991) The whole-body withdrawal response of *Lymnaea stagnalis*. I. Identification of central motoneurones and muscles. *J. Exp. Biol. 158,* 63–95.
7. Hatakeyama, D., Inamura, S., Ito, E., Sakakibara, M., Nelson, T. J., Alkon, D. L. (2004) Calexcitin-like immunoreactivity in the pond snail *Lymnaea stagnalis*. *Neurosci. Res. Comm. 35,* 32–40.
8. Kawai, R., Sunada, H., Horikoshi, T., Sakakibara, M. (2004) Conditioned taste aversion with sucrose and tactile stimuli in the pond snail *Lymnaea stagnalis*. *Neurobiol. Learn. Mem. 82,* 164–168.
9. Kuzirian, A. M., Epstein, H. T., Buck, D., Child, F. M., Nelson, T., Alkon, D. L. (2001) Pavlovian conditioning-specific increases of the Ca^{2+}- and GTP-binding protein, calexcitin in identified *Hermissenda* visual cells. *J. Neurocytol. 30,* 993–1008.

10. Kuzirian, A. M., Epstein, H. T., Gagliardi, C. J., Nelson, T. J., Sakakibara, M., Taylor, C., Scioletti, A. B., Alkon, D. L. (2006) Bryostatin enhancement of memory in *Hermissenda*. *Biol. Bull. 210,* 201–214.
11. Nelson, T. J., Alkon, D. L. (1995) Phosphorylation of the conditioning-associated GTP-binding protein cp20 by protein kinase C. *J. Neurochem. 65,* 2350–2357.
12. Ono, M., Kawai, R., Horikoshi, T., Yasuoka, T., Sakakibara, M. (2002) Associative learning acquisition and retention depends on developmental stage in *Lymnaea stagnalis*. *Neurobiol. Learn. Mem. 78,* 53–64.
13. Ridgway, R. L., Syed, N. I., Lukowiak, K., Bulloch, A. G. (1991) Nerve growth factor (NGF) induces sprouting of specific neurons of the snail, *Lymnaea stagnalis*. *J. Neurobiol. 22,* 377–390.
14. Sakakibara, M. (2006) Comparative study of visuo-vestibular conditioning in *Lymnaea stagnalis*. *Biol. Bull. 210,* 298–307.
15. Sakakibara, M., Aritaka, T., Iizuka, A., Suzuki, H., Horikoshi, T., Lukowiak, K. (2005) Electrophysiological responses to light of neurons in the eye and statocyst of *Lymnaea stagnalis. J. Neurophysiol. 93,* 493–507.
16. Sakakibara, M., Kawai, R., Kobayashi, S., Horikoshi, T. (1998) Associative learning of visual and vestibular stimuli in *Lymnaea*. *Neurobiol. Learn. Mem. 69,* 1–12.
17. Sakakibara, M., Okuda, F., Nomura, K., Watanabe, K., Meng, H., Horikoshi, T., Lukowiak, K. (2005) Potassium currents in isolated statocyst neuron and RPeD1 in the pond snail, *Lymnaea stagnalis*. *J. Neurophysiol. 94,* 3884–3892.
18. Syed, N. I., Winlow, W. (1991) Coordination of locomotor and cardiorespiratory networks of *Lymnaea stagnalis* by a pair of identified interneurones. *J. Exp. Biol. 158,* 37–62.